Frontiers in Heat and Mass Transfer (FHMT), 17, 5 (2021)
DOI: 10.5098/hmt.17.5

Global Digital Central
ISSN: 2151-8629

Frontiers in Heat and Mass Transfer

Available at www.ThermalFluidsCentral.org

NUMERICAL ANALYSIS OF A PROTOTYPE PUMP AS TURBINE AT DIFFERENT WORKING CONDITIONS

Xiao Sun [a,1] Fan-Kang Zeng [a], Jia-Bing Yang [a], Feng-Lin Zhou [a], Yu-Liang Zhang [b,*]

[a] *School of Mechanical Engineering, Hunan University of Technology, Zhuzhou, 412007, China*
[b] *College of Mechanical Engineering, Quzhou University, Quzhou, 324000, China*

ABSTRACT

In order to better study the internal flow characteristics of centrifugal pump as turbine, CFX software is employed to carry out numerical simulation to obtain flow field under different working conditions for pump as turbine based on the standard *k* - epsilon turbulence model and the SIMPLEC algorithm. The efficiency curves of the pump and pump as turbine are obtained under different working conditions. The results show that the effciency characteristics of the pump change greatly during the process of pumping. The efficiency of the turbine is higher than that of the pump under the respective optimal operating conditions. The internal flow characteristics of a turbine change greatly with the change of flow. By analyzing the related parameters in the internal flow structure, the internal characteristics of the turbine under different flow conditions are showed.

Keywords: *Centrifugal pump, Pump as turbine, Numerical calculation, Internal flow characteristic*

1. INTRODUCTION

In recent years, due to the shortage of traditional energy and serious environmental pollution and other problems, the development and use of secondary energy has attracted wide attention. Pumps inversion as energy recovery hydraulic turbine (PAT) is a hot research direction in the hydraulic machinery industry at home and abroad in recent decades. It has simple structure, low price, and convenient inspection and maintenance. More of these products have been put into actual production, and better economic benefits have been achieved (Wang et al., 2014). The internal flow field of centrifugal pump will change greatly during the process of inversion turbine. By comparing the external characteristics of pump and turbine and analyzing its internal flow structure, it can provide certain reference for turbine research and related production practice.

Derakhshan et al. used the "area ratio" method proposed by Burton to obtain the calculation formula of turbine efficiency through theoretical calculation (Derakhshan et al., 2008). Through the test of a centrifugal pump with medium specific speed, it is found that the test result is higher than the theoretical calculation. The author believes that the reason for the error is that the loss of the over-current components in the internal passage is not completely and accurately analyzed in the calculation process. By analyzing the test data, Nautiyal et al. deduced the formula for predicting turbine performance with the maximum pump efficiency and specific speed parameters (Nautiyal et al., 2011). Jain et alcarried out an experimental study on the influence of inlet diameter of the impeller (Jain et al., 2015), circle modification of inlet edge of the blade and rotation speed on turbine performance. Through regression analysis, the empirical coefficient expression of turbine efficient point parameter prediction was given, which further improved the prediction accuracy to within 10%.

Yang et al. mentioned in the literature that the numerical calculation can predict the performance parameters of the turbine more accurately (Yang et al., 2012). Near the design condition, the relative difference between the predicted value and the test value is the smallest, while in the low flow condition and the large flow condition, the relative difference between the predicted value and the test value is relatively large. Miao et al. used the numerical calculation method to study the performance difference of pumps with different flow-increasing designs (Miao et al., 2016), and obtained the parameter conversion coefficient of pump conditions and turbine conditions. Yang et al. carried out numerical calculation for three pumps with different specific revolutions as turbines. Based on dimensional analysis, combined with polynomial fitting method, a selection method suitable for centrifugal pumps as turbines was proposed (Yang et al., 2010). Literature(Yang et al., 2014) focused on the effect of the gap between the impeller and the volute on the performance and pressure pulsation of the pump. The results showed that with the increase in gap, the efficiency of the pump turbine shows a gradual increase after the optimal point. Moreover, the amplitude of the high-frequency pressure pulsation in the volute shows a decreasing trend, whereas that of the low-frequency pressure pulsation in the impeller remains basically unchanged. The essence is that the upstream influence of the incoming flow is large, and the downstream influence is small. Literature (Yang et al., 2011) designed three different blade shapes according to different blade inlet and wrap angles. The numerical results showed that when the small blade inlet angle and the large blade wrap angle are used, the efficiency of the optimal point is the highest; when the flow rate is greater than the design flow rate, the larger the wrap angle and the more evident the decrease in turbine efficiency become. In short, these studies provides an important reference for the research on other flow behavior of other fluid (Sampath et al., 2021), Li et al., 2021) .

To sum up, scholars have studied the performance of pump and turbine by combining theoretical analysis, numerical calculation and experiment, and given corresponding performance prediction formulas and selection methods. In this paper, a centrifugal pump with a low specific speed was used for turbine numerical calculation through CFD

* Corresponding author: zhang002@sina.com

technology, its external characteristic curve was drawn, and the internal flow field of the pump was compared and analyzed under different flow conditions during the inversion process.

2. MODEL AND METHOD

2.1 Calculation Model

The rated parameters of the centrifugal pump are as follows: flow Q=25m^3/h, head h=12.5m, and speed n=1450r/min. Inlet diameter of turbine impeller D_1=202mm, inlet placing Angle β_1=78°, inlet width of impeller b_2=9mm, inlet placing Angle β_2 =46°, outlet diameter of impeller D_2=76mm, volute base circle diameter D_3=210mm, outlet width of volute b_3=25mm, outlet diameter of volute D_4=48mm, number of blades Z=6.The computational domain is shown in Fig.1. The mesh sensitivity study is carried out with 5 grid numbers, it is found that the pump head correlation is less than 1% and there is almost no difference among the flow fields when the final grid number is 1194160 grids. Consequently, the influence of the grid numbers on the numerical results can be ignored. The number of impeller grids is 480612 and the number of volute grids is 455152.

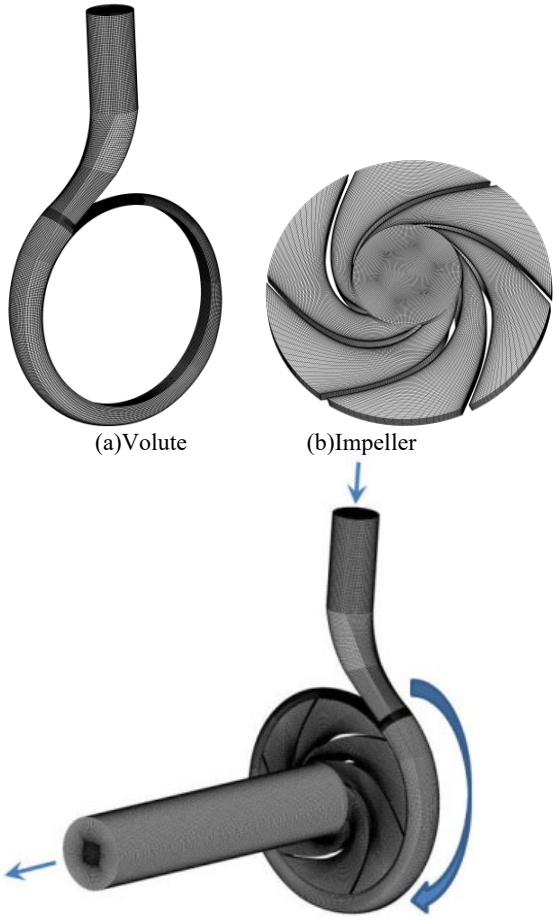

(a)Volute (b)Impeller

(c)Total calculation region

Fig. 1 Schematic diagram of hydraulic turbine calculation domain model

2.2 Calculation Method

In this paper, the commercial fluid computing software ANSYS CFX is used to calculate the fluid computational domain.

The inlet boundary condition of the hydraulic turbine is set as the constant pressure inlet, and the outlet boundary condition is set as the mass flow rate. The connection area between the outlet section and the impeller and the interface between the impeller and the volute is set as the interface. The pressure solver is adopted, and the convergence precision is set as 10-5. There is no slip on the impeller surface and other wall surfaces. The SIMPLEC algorithm and k-epsilon turbulence model were used for the corresponding calculation. The conveying medium is the clear water medium at room temperature, the density is 998.2kg/m^3.

3. CALCULATION RESULTS

3.1 Monitoring Point

In order to explore the pressure distribution of each flow field at the highest efficiency point of the pump and pump-driven turbine, the points shown in Fig. 2 are taken as the monitoring points. Fig.3 shows the calculated efficiency curve of the pump and the pump turbine. It can be seen that the maximum efficiency of the turbine is 78.1%, and the corresponding flow rate is 32.5m^3/h. The high efficiency zone of the turbine is wider than that of the pump.

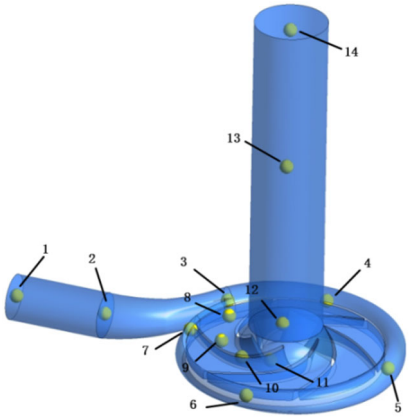

Fig. 2 Position of each monitoring point

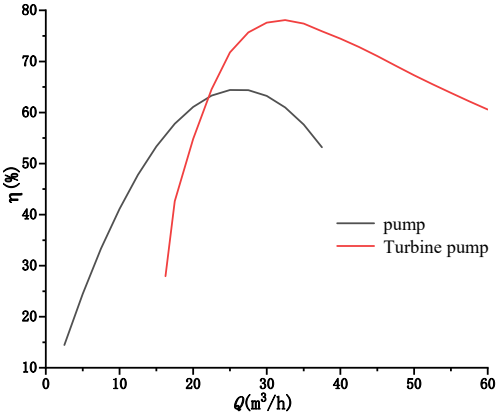

Fig. 3 Pump and pump turbine efficiency curve

In order to compare the internal flow of the pump and the turbine at the highest efficiency, the inlet pressure of the pump is set as 1atm, the outlet pressure of the pump is the mass flow rate, and the outlet pressure of the pump is the inlet condition of the turbine. Figure 4 shows the static pressure distribution at each monitoring point.

It can be seen that when the efficiency reaches the highest point, the pressure difference between the static pressure of the pump and the turbine is larger near the inlet of the turbine. The maximum value is about 60kPa.In the impeller and volute area, the static pressure inside the pump and turbine has little difference, and the static pressure inside the pump is slightly higher than that inside the turbine. The pressure difference between the pump and the turbine at the monitoring points 8, 9 and 10 is large along the direction of the blade extension, which reflects that there is a large pressure difference in the blade rotation

area. At the tail pipe of the turbine, the pressure of the two is basically the same, about 90kPa.Near the volute, the static pressure of the pump and the turbine is basically the same, about 220kPa.

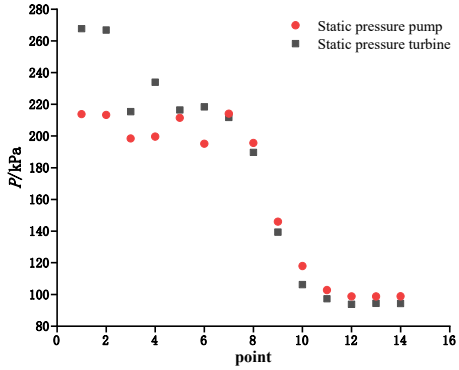

Fig. 4 Static pressure distribution at each monitoring point

Fig. 5 shows the velocity distribution at each monitoring point. It can be seen that the pump speed is generally lower than that of the turbine. The average speed of each pump point is 5.20m/s, and the average speed of each turbine point is 6.83m/s. The maximum velocity of the pump and turbine is 10.47m/s and 11.31m/s at the monitoring point 8 and 3, respectively. At the monitoring point 7, the two velocities are greatly affected by the cochlear tongue. From the turbine inlet to the volute passage, the velocity increases gradually as the volute passage area decreases. At the tail pipe, the velocity changes little and the pump and turbine speed are the same, about 2.0m/s. At the monitoring points 1 and 10, the speed of pump and turbine is basically the same, about 5.0m/s. The velocity difference at the monitoring points 8, 9 and 10 in the impeller area is large and decreases gradually, indicating that the velocity decreases gradually along the blade extension direction.

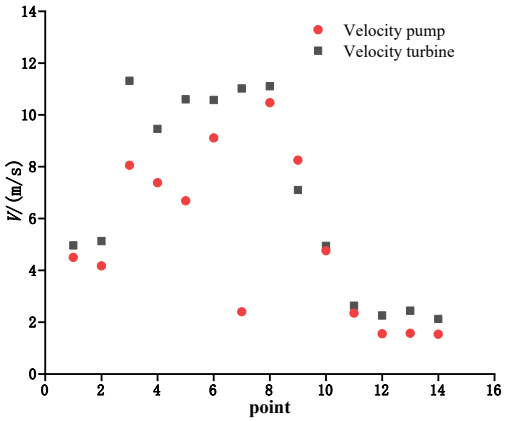

Fig. 5 Velocity distribution at each monitoring point

3.3 Internal Flow Field

In this study, the total inlet pressure was set at 28kPa. By CFD numerical calculation, the pressure, velocity, turbulent kinetic energy and turbulent dissipation rate of the turbine under low flow conditions ($0.7Q_t$), optimal flow conditions (Q_t) and large flow conditions ($1.3Q_t$) were respectively obtained. The internal flow characteristics of the turbine under different flow conditions were compared and analyzed.

Fig. 6 shows the pressure cloud diagram of the middle section of the hydraulic turbine under three working conditions. As can be seen from the figure, the stratification of a turbine under the optimal flow condition is more obvious than that under other flow conditions. From the inlet to the cochlea tongue, the pressure of the turbine is divided into four layers under the optimal working condition, and the pressure value decreases from 280kPa to 186kPa. The pressure from the inlet of the turbine blade (trailing edge of the pump blade) to the outlet of the turbine impeller is divided into six layers and evenly distributed. Under low flow conditions, the pressure from the inlet to the tongue of the turbine can be divided into three layers with high pressure, while under high flow conditions, the stratification in the impeller area is not obvious. Under the three flow conditions, the static pressure at the tongue is about 201~216kPa, 165~186kPa and 96.4~130kPa, respectively. It can be seen that with the increase of flow rate, the static pressure at the cochlea tongue gradually decreases. Under three flow conditions, the pressure values at the outlet of the hydraulic turbine are 127kPa, 58.6kpa and -73.2kpa, respectively. The mean static pressure in the impeller area is about 167kPa, 113kPa and 28kPa, respectively. It can be seen that with the increase of flow rate, the pressure difference inside the turbine increases gradually. Along the extension direction of turbine blade, when the relative length is 0.5-1, the pressure between the two blades is 127~156kPa, 58~101kPa and -73.2~ -5.4kPa respectively under the three working conditions. It can be seen that the low pressure area is widely distributed under the condition of large flow. In addition, under low flow conditions, the dynamic and static interference of the inner wall of the volute is higher than other conditions.

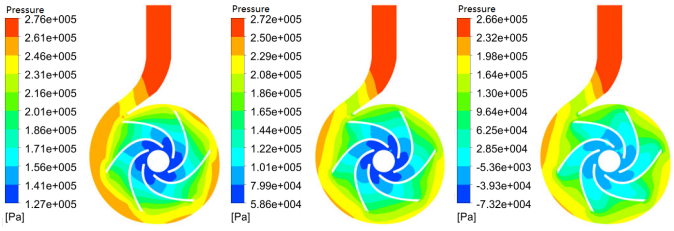

Fig. 6 Hydraulic turbine pressure distribution diagram under three different flow rates a)Low flow condition; b)Optimal flow condition; c)Large flow condition

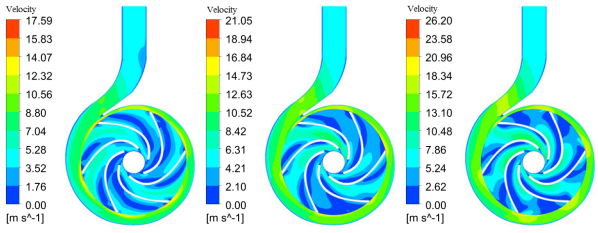

Fig. 7 Hydraulic turbine velocity distribution diagram under three different flow rates a)Low flow condition; b)Optimal flow condition; c)Large flow condition.

Fig. 7 shows the velocity distribution of the turbine under different flow conditions. It can be seen from figure7 that in the whole flow field, the interface between the impeller and the volute reaches the maximum velocity value. The maximum flow rate is 17.59m/s under low flow conditions, 21.05m/s under optimal conditions, and 26.20m/s under high flow conditions. It can be seen that with the increase of flow rate, the maximum value of fluid velocity in the passage increases. Under low flow conditions, the flow rate in most areas of the volute is between 5.28 and 12.32m/s. Under the optimal working condition, the velocity of most areas of the volute is between 6.31 and 14.73m/s. Under high flow conditions, the flow rate in most areas of the volute is between 7.86 and 18.34m/s. In the whole impeller area, the velocity of the working surface is lower than that of the back surface. The lowest flow rate on the blade is within the range of 0~0.5 of the relative length of the working face of the blade, where swirls tend to form, which affects the hydraulic efficiency of the turbine. It can be seen from the comparison that the velocity distribution range in the blade area is relatively narrow under low flow conditions, and the fluid is greatly affected by inertia.Fig.8 shows the velocity streamline distribution of

the turbine under different flow rates. It can be seen that vortex regions are generated in the turbine under three working conditions, and there are more vortex regions under low flow conditions and large flow conditions. Under the low flow condition, the vortex area of turbine is mainly concentrated on the blade working face. The vortex area under the high flow condition is mainly concentrated on the back of the blade. Under the optimal flow condition, the velocity streamline is basically the same as the bending direction of the blade, and there are fewer eddies. It can be seen that the hydraulic loss caused by flow inertia under the optimal flow condition is small.

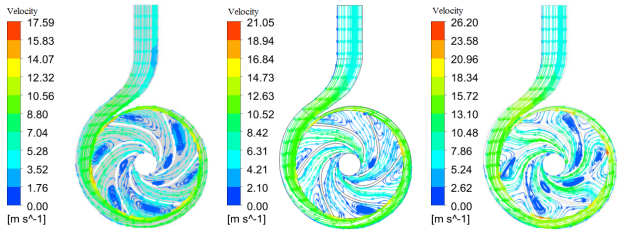

Fig.8 Turbulence energy curves of hydraulic turbines at different flow rate a)Low flow condition; b)Optimal flow condition; c)Large flow condition

Fig. 9 shows the volume-weighted average distribution of turbulent flow energy of a hydraulic turbine under different flow conditions. It can be seen from the figure that, with the growth of flow, the turbulence intensity of turbines first increases, then slightly decreases, and then gradually increases. At $0.5Q_t$, the turbulent kinetic energy is $0.17m^2/s^2$, and at $1.3Q_t$, it is $0.52m^2/s^2$.It can be seen that the turbulence kinetic energy increased by $0.35m^2/s^2$ within the range of $0.5Q_t$ ~$1.3Q_t$. At flow rates of $0.5Q_t$, $0.7Q_t$, $0.9Q_t$,1.1 Q_t,$1.3Q_t$, and $1.5Q_t$, the growth rate of turbulent kinetic energy (the growth rate of turbulent kinetic energy per unit variable flow) is 0.040, -0.004, 0.010, 0.022, and 0.035, respectively. Under low flow conditions, the turbulent kinetic energy changes slowly. As traffic increases, its growth rate accelerates. The turbulence kinetic energy changes very little when the flow is between $0.5Q_t$ and Q_t. In order to observe the distribution of turbulent kinetic energy under different flow rates, the axial surfaces of the blades and the middle sections of the whole flow field under three working conditions were taken for analysis.

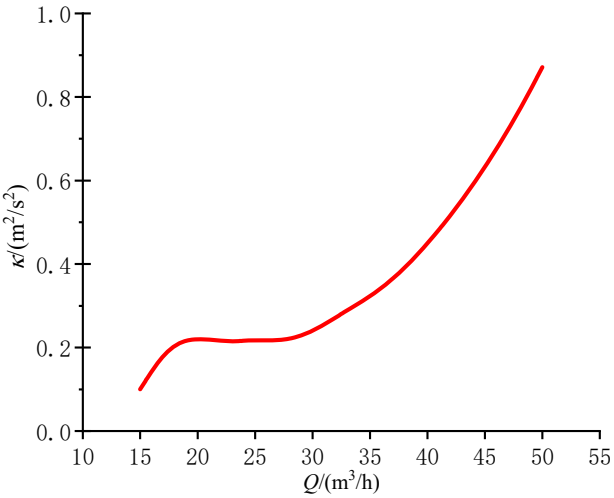

Fig. 9 Turbulence kinetic energy curves of hydraulic turbines at different flow rates

Fig. 10 shows the distribution of turbulent kinetic energy in the impeller area under three different flow conditions. In Fig.10 (a), (b), and (c), the average volume of turbulent kinetic energy of the impeller is $0.72m^2/s^3$, $0.61m^2/s^3$, and $1.02m^2/s^3$, respectively. It can be seen from the figure that the turbulent kinetic energy of the turbine impeller is the largest at the inlet, where there is obvious stratification phenomenon. Under three flow conditions, the maximum turbulent kinetic energy of the impeller is $6.0m^2/s^2$, $4.8m^2/s^2$ and $6.4m^2/s^2$, respectively. The turbulent kinetic energy near the inlet was 1.2~$6.0m^2/s^2$,1.1~$4.8m^2/s^2$ and 1.5~$6.4m^2/s^2$, respectively. Under the three flow conditions, the boundary between the impeller and the outlet is accompanied by a large turbulent kinetic energy, which is slightly lower than the inlet interface, respectively 0.2~$0.7m^2/s^2$, 0.4~$0.9m^2/s^2$, and 0.6~$2.4m^2/s^2$. It can be seen that the turbulent kinetic energy increases layer by layer along the blade wall, and the larger the flow, the greater the turbulent kinetic energy.

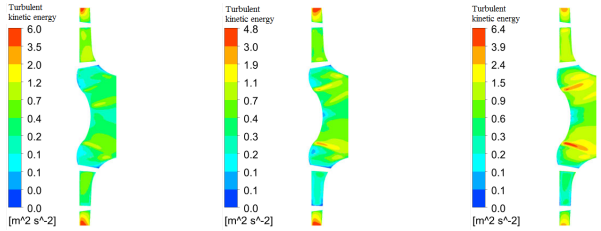

Fig. 10 turbulent kinetic energy distribution of impeller under three different flow rates a)Low flow condition; b)Optimal flow condition; c)Large flow condition

Fig. 11 shows the distribution of turbulent kinetic energy of the hydraulic turbine under three flow rates. As can be seen from the figure, the turbulent kinetic energy is the strongest near the cochlea tongue in the whole flow field. The maximum turbulent kinetic energy under the three working conditions is $6.53m^2/s^2$, $9.89m^2/s^2$ and $16.30m^2/s^2$, respectively. It can be seen that with the increase of flow rate, the maximum turbulent kinetic energy of the flow field inside the turbine increases. In the inlet passage, the turbulent kinetic energy of the flow field is basically unchanged and very small, whose value is 0~0.66 m^2/s^2.The turbulence kinetic energy value is small under the condition of small flow, but the distribution area is wide and the distribution of each blade is relatively uniform, and its size is 0.66~$4.57m^2/s^2$.Under the optimal condition, the turbulent kinetic energy is mainly distributed on the blade near the cochlea tongue, whose size is 1.98~3.96 m^2/s^2. Under the condition of large flow, the distribution of turbulent kinetic energy is concentrated, mainly near the outlet of turbine blade, and its size is 3.26~6.52 m^2/s^2. In addition, the turbulent kinetic energy of the blade working face is lower than that of the blade working face under the condition of large flow.

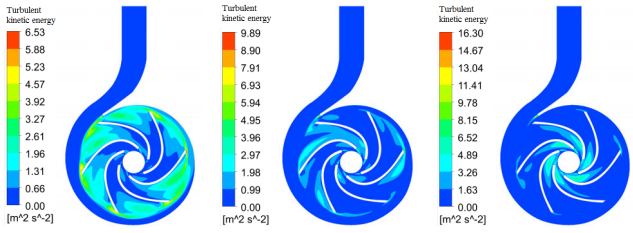

Fig. 11 Turbulent kinetic energy distribution of hydraulic turbines under three different flow rates a)Low flow condition; b)Optimal flow condition; c)Large flow condition

Fig.12 shows the curves of turbulent dissipation rate of hydraulic turbine under different flow rates. As can be seen from the figure, with the increase of flow rate, the turbulent dissipation rate of the hydraulic turbine increases first, then decreases and then increases. The change has some similarity with turbulent kinetic energy. When the flow is $0.5Q_t$, $0.7Q_t$, $0.9Q_t$, $1.1Q_t$, $1.3Q_t$ and $1.5Q_t$, the turbulence dissipation

rate is 38.04m^2/s^3, 48.58m^2/s^3, 50.37m^2/s^3, 73.76m^2/s^3, 123.33m^2/s^3 and 211.77m^2/s^3, respectively. At flow rates of 0.5Q_t, 0.7Q_t, 0.9Q_t, 1.1Q_t, 1.3Q_t and 1.5Q_t, the growth rate of turbulent kinetic energy (the increase of turbulent dissipation rate per unit variable flow) was 7.51,-0.75, 1.83, 5.39, 10.26 and 16.93, respectively. At low flow conditions, the turbulent kinetic energy changed slowly. As traffic increases, its growth rate accelerates. The turbulence dissipation rate changes very little when the flow is between 0.5Q_t and Q_t. In order to observe the distribution of turbulent dissipation rate of turbine under different flow rates more carefully, the axial surface of blade and the middle section of the whole flow field under three working conditions were taken for analysis.

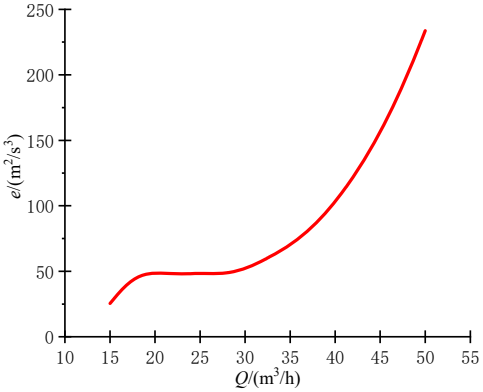

Fig. 12 Turbulence dissipation rate curves of hydraulic turbines at different flow rates

Fig.13 shows the distribution of turbulent dissipation rate in the impeller area under three different flow conditions. In figure 10(a), (b), and (c), the average volume of turbulent kinetic energy of the impeller is 173m^2/s^3, 175m^2/s^3, and 352m^2/s^3, respectively. It can be seen from the figure that the turbulent kinetic energy of the turbine impeller is the largest at the inlet, where there is obvious stratification. Under three flow conditions, the turbulent kinetic energy near the inlet is 2.4×10^2~3.8×10^{3}m^2/s^3, 1.4×10^2~1.2×10^{3}m^2/s^3, and 1.4×10^2~3.8×10^3 m^2/s^3, respectively. Under three flow conditions, the boundary between the impeller and the outlet is accompanied by a large turbulence dissipation rate, whose values are respectively 0~4.1×10^{2}m^2/s^3, 2.4×10^2~3.8×10^3 m^2/s^3, 2.4×10^{2}m^2/s^3~1.1×10^{4}m^2/s^3. It can be seen that the turbulent kinetic energy increases layer by layer along the blade wall, and the larger the flow, the higher the turbulent dissipation rate.

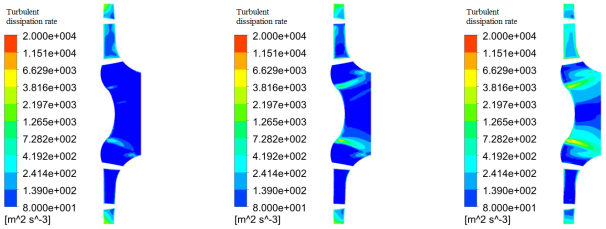

Fig. 13 Turbulent kinetic energy distribution of hydraulic turbines under three different flow rates a)Low flow condition; b)Optimal flow condition; c)Large flow condition

Fig.14 shows the distribution of turbulent dissipation rate of the hydraulic turbine under three different flow conditions. Due to the large numerical range and uneven distribution of turbulence dissipation rate, the turbulence dissipation rate within the range of 0~1200m^2/s^3 was taken as the observation object. The turbulence values in this range cover most areas of the internal flow field. It can be seen from the figure that the turbulent dissipation rate in the flow field is larger at the tongue of the cochlea and the head and tail of the blade. The image is similar to the image of turbulent kinetic energy. Under low flow conditions, the turbulent dissipation rate in most areas of the impeller is 240~360m^2/s^3.Under the optimal flow condition, the turbulent dissipation rate in most areas of the impeller is 360~480m^2/s^3.Under the condition of large flow, the turbulent dissipation rate in most areas of the impeller is 480~960m^2/s^3.It can be seen that the turbulence dissipation rate increases with the increase of flow. In addition, with the increase of flow rate, the turbulence dissipation rate tends to move towards the outlet of the turbine and the value of turbulence dissipation rate near the outlet increases.

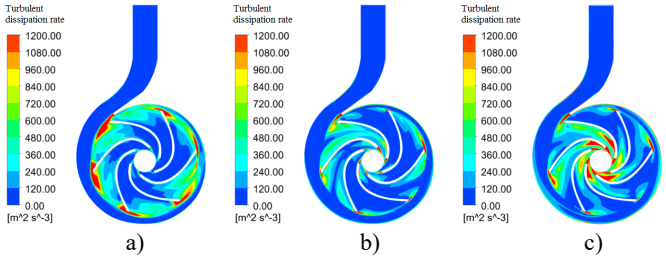

Fig. 14 Turbulent kinetic energy distribution of hydraulic turbines under three different flow rates: a) Low flow condition; b) Optimal flow condition; c) Large flow condition

4. CONCLUSION

In this paper, the designed centrifugal pump and pump turbine were numerically calculated by CFX software, and the external characteristics of the pump and turbine, as well as the internal flow characteristics of the turbine, such as pressure, velocity, turbulent kinetic energy and turbulent dissipation rate, were obtained under low flow conditions (0.7Q_t), optimal flow conditions (Q_t) and large flow conditions (1.3Q_t). By comparing its internal characteristics, the relevant conclusions can be drawn. The results show:

1) after the centrifugal pump is inverted as a turbine, its head, efficiency and power all change greatly. Among them, the head change is the biggest, both in the optimal working condition, turbine efficiency is higher than pump efficiency.

2) turbine performance changes greatly under different flow conditions. With the increase of flow rate, the pressure difference, velocity, turbulent kinetic energy and turbulent dissipation rate increase. The pressure and velocity are stratified obviously and the effect of static and static interference is small.

3) through the observation of the internal flow images, it can be seen that the pressure, velocity, turbulent kinetic energy and other parameters in the impeller region change significantly, and the impeller part has a large energy change and pressure loss, so the research on this region needs to be in-depth.

ACKNOWLEDGEMENTS

The research was financially supported by the National Natural Science Foundation of China (Grant No.51876103, No. 51976202).

NOMENCLATURE

Q	flow (m^3/h)
h	head (m)
n	speed(r/min)
D_1	Inlet diameter of turbine impeller (mm)
β_1	inlet placing Angle
b_2	inlet width of impeller (mm)
β_2	inlet placing Angle
D_2	outlet diameter of impeller (mm)
D_3	volute base circle diameter (mm)
b_3	outlet width of volute (mm)
D_4	outlet diameter of volute (mm)
z	number of blades

REFERENCES

Wang, X. H., Yang, J. H., and Shi, F. X., 2014, "Research status and prospect of energy recovery hydraulic turbine," *Journal of Drainage and Irrigation Machinery Engineering*, **32**(09), 742-747. http://dx.doi.org/10.3969/j.issn.1674-8530.14.0115

Derakhshan, S., Nourbakhsh, A., 2008, "Theoretical, numerical and experimental investigation of centrifugal pumps in reverse operation," *Experimental Thermal and Science Fluid*, **32**(8), 1620-1627. http://dx.doi.org/10.1016/j.expthermflusci.2008.05.004

Nautiyal, H., Varun, K.A., Yadav, S., 2011, "Experimental investigation of centrifugal pump working as turbine for small hydropower systems," *Energy Science and Technology*, **l**(1), 79-86. http://dx.doi.org/10.3968/j.est.1923847920110101.006

Jain, S., Swarnkar, A., Motwani, K., et al., 2015, "Effects of impeller diameter and rotational speed on performance of pump running in turbine mode," *Energy Conversion and Management*, **89**, 808-824. http://dx.doi.org/10.1016/j.enconman.2014.10.036

Yang, S. S., Kong, F. Y., Su, X. H., et al, 2012, "Numerical simulation and external characteristic experiments of pump s and pumps used as turbines," *Journal of Xi'an JT University*, **3**(46), 36-41. http://dx.doi.org/CNKI:61-1069/T.20120224.1036.005

Miao, S. C, Yang, J. H., Sun, Y. J., et al, 2016, "Research on selection of hydraulic turbine," *Journal of Xihua University (Natural Science Edition)*, **35**(6), 23-26. http://dx.doi.org/10.3969/j.issn.1673-159X.2016.06.005

Yang, J. H., Yuan, Y. F., Jiang, Y. G., et al, 2010, "Performance prediction of centrifugal pump reversing as an energy recovery turbine," *Journal of Lanzhou University of Technology*, **1**(36), 54-56. http://dx.doi.org/10.3969/j.issn.1673-5196.2010.01.013

Yang, S. S., Liu, H. L., Kong, F. Y., et al, 2014, "Effects of the radial gap between impeller tips and volute tongue influencing the performance and pressure pulsations of pump as turbine," *Journal of Fluids Engineering*, **136**, 054501-1-8. http://dx.doi.org/10.1115/1.4026544

Yang, J. H., Wang, X. H., 2011, "Effect of vane profile on hydraulic energy recovery turbines performance," J*ournal of Drainage and Irrigation Machinery Engineering*, **29**(4), 287-291. (in Chinese with english abstract) http://dx.doi.org/10.3969/j.issn.1674-8530.2011.04.003

Sampath Kumar, V.S., Pai, N.P., Devaki, B.,2021, "Analysis of MHD flow and heat transfer of laminar flow between porous disks," *Frontiers in Heat and Mass Transfer*, **16**(3), 1. http://dx.doi.org/10.5098/hmt.16.3

Li, J., Zhang, Y. B., 2021, "Flow equations and their borderlines for different regimes of mass transfer," *Frontiers in Heat and Mass Transfer*, **16**(21), 1. http://dx.doi.org/10.5098/hmt.16.21